



# Characterization of Cosmic Grain Analogs Formed at Low Temperature from Small Hydrocarbon Precursors in the NASA Ames COSmIC Facility

Ella Sciamma-O'Brien  and Farid Salama 

NASA Ames Research Center, Space Science & Astrobiology Division, Moffett Field, CA 94087, USA; [ella.m.sciammaobrien@nasa.gov](mailto:ella.m.sciammaobrien@nasa.gov)  
Received 2020 April 18; revised 2020 September 29; accepted 2020 October 7; published 2020 December 10

## Abstract

Here, we present the results of the first solid-phase ex situ analysis of cosmic grain analogs produced at low temperature ( $<200$  K) in the NASA Ames COsmic Simulation Chamber (COSmIC) from small hydrocarbon precursors, methane ( $\text{CH}_4$ ) and acetylene ( $\text{C}_2\text{H}_2$ ), seeded in an argon supersonic jet expansion and submitted to a plasma discharge. The plasma-induced chemical reactions, initiated between the precursor molecules and their atomic and molecular fragments, radicals and ions, produce larger molecules and eventually solid particles that are collected in situ under controlled conditions. Scanning electron microscopy (SEM) imaging was used to provide insight on the morphology and growth structure of the grains produced in COSmIC, and to investigate how the precursors used to produce the grains affect these parameters. This SEM study has shown that under identical experimental conditions with fixed physical and chemical parameters (precursor density, temperature, energy, and reaction time), heavier precursors in the initial mixture produce larger grains and in larger quantity, most likely as a result of a more complex chemistry: most of the grains produced in the Ar/ $\text{CH}_4$  (95:5) gas mixture ranged from 15 to 385 nm in diameter with an average density of  $2.1 \text{ grains } \mu\text{m}^{-2}$ , while the grains produced in the Ar/ $\text{C}_2\text{H}_2$  (95:5) gas mixture ranged from 40 to 650 nm with a density of  $3.5 \text{ grains } \mu\text{m}^{-2}$ . Changes in the morphology were also observed, with grains produced from acetylene ( $\text{C}_2\text{H}_2$ ) precursors tending to be more spherical than grains produced from methane ( $\text{CH}_4$ ) precursors. This change in morphology could be associated with different stages of growth formation at low temperature from a more “planar” growth at first, followed by coagulation into more spherical particles. This study demonstrates that the COSmIC experimental setup can be used to investigate carbon grain formation from small gas-phase molecular precursors at low temperature ( $<200$  K), i.e., under a temperature regime that is representative of the dust condensation zone and outer region of circumstellar envelopes.

*Unified Astronomy Thesaurus concepts:* [Laboratory astrophysics \(2004\)](#); [Experimental techniques \(2078\)](#); [Carbonaceous grains \(201\)](#); [Circumstellar grains \(239\)](#)

## 1. Introduction

Cosmic dust is ubiquitous in the universe. It plays a major role in our understanding of a broad range of astrophysical processes ranging from stellar mass loss to planetary system formation. Understanding the formation processes and the evolution of cosmic dust grains from the circumstellar envelopes (CSEs) of late-type stars to the diffuse interstellar clouds, to the dense interstellar clouds and, ultimately, to planetary systems provides important insights into the properties of these astrophysical objects. The CSEs of asymptotic giant branch (AGB) stars are known to be efficient sites for molecule and dust grain formation and are considered to be among the main sources of interstellar dust (Henning & Salama 1998). The nature of the molecules and dust grains found in CSEs is largely defined by the carbon-to-oxygen (C/O) abundance ratio at the photosphere of the AGB stars with most of the available carbon in oxygen-rich stars (M-type,  $\text{C/O} < 1$ ) locked in CO molecules, while most of the oxygen in carbon-rich stars (C-type,  $\text{C/O} > 1$ ) is locked in CO molecules (Massalkhi et al. 2019). As a result, the molecules and dust formed in M-type star envelopes are predominantly oxygen-bearing molecules and silicate dust, while those formed in C-rich star envelopes are predominantly carbon-bearing molecules with carbonaceous-, primarily silicon carbide (SiC), and magnesium sulfide dusts. In all cases, the proposed mechanism for dust grain formation is that gas-phase precursors first condense near the surroundings of the stellar photosphere (Gail & Sedlmayr 2013); and these condensation

nuclei then grow to micrometer sizes as a consequence of accretion and coagulation processes.

Little is known, however, about the physical and chemical processes that drive the formation of dust grains from gas-phase molecular precursors. Various theoretical mechanisms have been proposed to describe the formation processes that go from small hydrocarbons to polycyclic aromatic hydrocarbons (PAHs) and to carbon dust in astrophysical environments (Frenklach & Feigelson 1989; Allain et al. 1997; Herpin et al. 2002; Cau 2002, Draine 2003, Cherchneff 2011), and laboratory experiments have been developed to investigate the formation of carbonaceous dust grains using combustion flames, UV photolysis, laser ablation and pyrolysis, and plasma discharges as the energy source (Bréchignac et al. 2005; Kovacevic et al. 2005; Jäger et al. 2006, 2009; Lee et al. 2007; Arnas et al. 2009; Biennier et al. 2009; Contreras & Salama 2013; Contreras et al. 2014; NASA press release 2014; Fulvio et al. 2017; Hodoroaba et al. 2018; Peláez et al. 2018). Laboratory astrophysics is essential in our understanding of these processes, although it is extremely difficult to reproduce the astrophysical environments in which dust forms. To the best of our knowledge, only a few laboratory experiments have been conducted in the gas phase under temperature conditions representative of the cold circumstellar environment: Contreras & Salama (2013) studied the gas-phase chemistry leading to the formation of cosmic grains from small hydrocarbons and PAHs at low temperatures below 200 K representative of the dust condensation zone and outer region of the CSE (NASA Press

Release 2014); and, more recently, Martínez et al. (2020) investigated the formation of grains from atomic sources at temperatures  $<1000$  K representative of the inner CSE, and Gavilan et al. (2020) investigated the formation of grains from PAH precursors at temperatures  $<200$  K representative of the dust condensation zone and outer region of the CSE.

The COSmic Simulation Chamber (COSmIC) was developed to generate, process, and analyze interstellar, circumstellar, and planetary analogs in the laboratory under low-temperature conditions representative of these environments (Salama et al. 2017). COSmIC has been used to study gas-phase hydrocarbons and PAHs and their chemical reactivity, as well as the formation of solid carbon grain particles under controlled low-temperature ( $<200$  K) and pressure ( $<30$  mbar) conditions representative of interstellar and circumstellar environments (Biennier et al. 2003; Tan & Salama 2006; Salama et al. 2011; Contreras & Salama 2013; Contreras et al. 2014; Bejaoui & Salama 2019, Gavilan et al. 2020), and as an experimental platform for the Titan Haze Simulation experiment to investigate the low-temperature complex organic chemistry occurring between nitrogen and methane in Titan's atmosphere and resulting in the formation of complex molecular gas-phase species and the subsequent production of solid aerosols (Ricketts et al. 2011; Sciamma-O'Brien et al. 2014, 2015, 2017; Raymond et al. 2018).

The COSmIC facility allows investigation of the formation mechanisms of carbonaceous dust grains found in envelopes around C-type stars as it permits the study of the carbon life cycle from small neutral and ionized hydrocarbons and PAH precursors in the gas phase to solid carbon grains. The gas-phase precursors and the products resulting from the plasma chemistry are studied in situ by reflectron time-of-flight mass spectrometry and cavity ring-down spectroscopy, while the solid-phase products (grain analogs) are deposited on substrates, collected under a controlled atmosphere, and analyzed ex situ using various analytical methods. Extensive in situ mass spectrometry studies of the gas phase have been conducted by Contreras & Salama (2013) and Sciamma-O'Brien et al. (2014) to monitor the chemistry in the gas phase. These studies have shown that only small molecular species containing up to two C-atoms are detected in the gas phase in Ar/CH<sub>4</sub> plasma expansions, while molecular species containing up to six C-atoms are detected in the gas phase in Ar/C<sub>2</sub>H<sub>2</sub> plasma expansions. These findings have been confirmed by a recent modeling study of the chemical reactivity in COSmIC (Raymond et al. 2018). For mixtures containing more complex precursors, Contreras & Salama (2013) observed chemical pathways that support the hydrogen abstraction and acetylene addition (HACA) mechanism (Frenklach & Wang 1994) for PAH growth through the sequential hydrogen abstraction and acetylene addition in argon-benzene, argon-pyridine, and argon-toluene plasmas. In addition, in an ex situ mass spectrometry analysis of cosmic grain analogs produced at low temperature in COSmIC from PAH precursors, Gavilan et al. (2020) demonstrated that molecular growth is possible at low temperature via the methyl addition-cyclization (MAC) mechanism (Shukla et al. 2008), suggesting that molecular growth and dust formation from PAHs is feasible at low temperatures in CSEs. These studies have demonstrated that COSmIC's unique design allows monitoring of specific chemical pathways associated with the presence of hydrocarbon precursors.

Here, we present the results of the ex situ analysis of cosmic grain analogs produced at low temperature in COSmIC from two different precursor gas mixtures: Ar/CH<sub>4</sub> (95:5) and Ar/C<sub>2</sub>H<sub>2</sub> (95:5). Scanning electron microscopy (SEM) imaging was used to provide insight on the morphology and growth structure of the grains produced in COSmIC, and to investigate how the precursors used to produce the grains affect these parameters. In the following sections, we briefly describe the experimental setup and present the ex situ SEM analysis performed on the COSmIC grains, before discussing the results.

## 2. Experimental

### 2.1. The COSmic Simulation Chamber

COSmIC is an experimental facility that was developed at NASA Ames to generate, process, and analyze interstellar, circumstellar, and planetary analogs in the laboratory (see Figure 1). The experimental setup and its different applications have been described previously (see Salama et al. 2017, for a review, and references therein). COSmIC consists of a pulsed discharge nozzle (PDN) coupled to a vacuum chamber to produce an adiabatic expansion that allows cooling down a gas mixture injected in the chamber at room temperature to astrophysically relevant temperatures (150–50 K) and reduce the pressure from  $\sim 500$  mbar down to  $\sim 30$  mbar in the plasma cavity (Broks et al. 2005). The pressure decreases further to 0.1 mbar in the stream of the expansion, past the electrodes. These temperature and pressure regimes are achieved by pumping a gas mixture through a set of two consecutive slits of increasing sizes (127  $\mu\text{m}$  then 400  $\mu\text{m}$  thick). The gas mixtures that have been studied have consisted of a carrier gas (Ar, N<sub>2</sub>) seeded with hydrocarbon gas-phase precursors (from small hydrocarbon molecules such as CH<sub>4</sub>, C<sub>2</sub>H<sub>2</sub>, and C<sub>6</sub>H<sub>6</sub> to PAHs). A plasma discharge generated by applying a high voltage ( $-800$  V) onto electrodes placed in the stream of the supersonic jet expansion can then be used to induce chemistry between the different precursor molecules present in the expansion. The chemistry occurs within the plasma cavity formed by the larger 400  $\mu\text{m} \times 10$  cm slit, in a 1.5 mm thick alumina dielectric plate separating the anode (the PDN body) from the cathodes (the Elkonite electrodes) where the gas temperature and pressure stabilize at 150 K and 30 mTorr, respectively (Broks et al. 2005; Biennier et al. 2006), before the plasma is turned on. The pressure achieved in this plasma cavity is higher than in the astrophysical environments we are simulating. However, this higher pressure is necessary in order to enhance the chemistry, for the chemical reactions resulting in the production of more complex molecular species and grains to occur in a laboratory timescale. The neutral and ionized precursors, their atomic and molecular fragments, as well as gas-phase products of the chemistry can be probed and monitored in situ in COSmIC using two highly sensitive diagnostics coupled to the PDN: a UV-visible-NIR cavity ring-down spectrometer (CRDS) and a reflectron time-of-flight mass spectrometer (ReTOF-MS). The complex chemistry induced by the plasma discharge not only results in more complex molecular gas-phase species but also produces solid particles that are the focus of the study presented here.

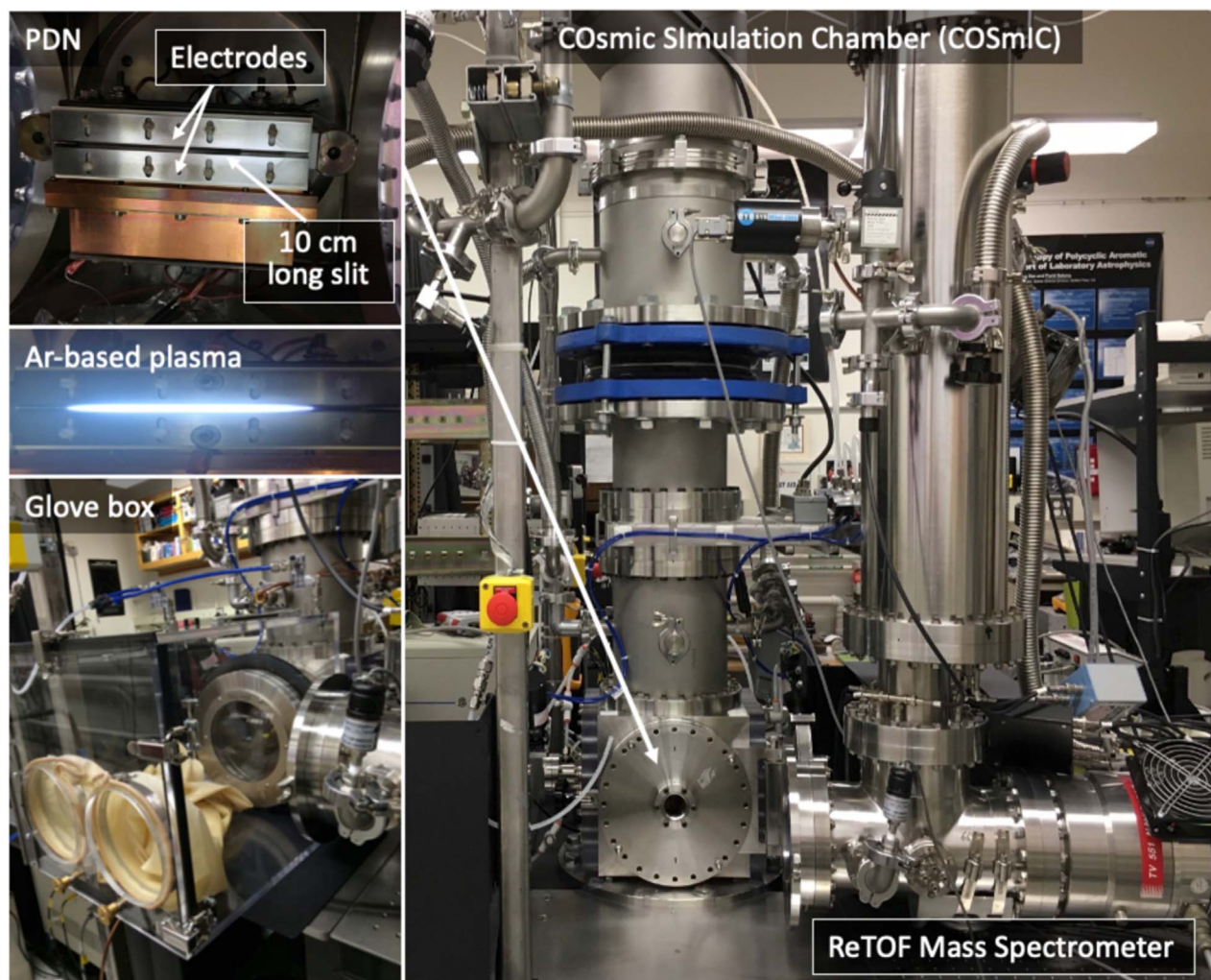


**Figure 1.** Right: the COSmIC experimental setup. Top left: the pulsed discharge nozzle (PDN) showing the slit through which the gas expands and the electrodes to generate the plasma. Middle left: the argon planar plasma expansion. Bottom left: the glove box used to remove the solid samples under controlled argon atmosphere to minimize exposure to air.

## 2.2. Production of Cosmic Grain Analogs

The gas-phase molecular species and solid particles produced in COSmIC are formed at low temperature ( $<200$  K) within the plasma cavity in the dielectric plate slit and are carried by the supersonic gas expansion past the electrodes where they encounter a sudden drop in pressure and temperature to 0.1 mbar and 50 K, respectively. The solid grains are then collected by jet deposition onto different substrates placed perpendicular to the flow, a few centimeters (typically 3–5 cm) downstream from the electrodes. Depending on the ex situ analysis to be performed, experiments can be run for as short as 1 hour or up to 40 hours. At the end of a deposition run, the vacuum chamber is brought back to base pressure (8 mTorr), and the chamber is filled with argon. Previous TOF measurements acquired at varying distances from the slit in the COSmIC setup (Contreras & Salama 2013) have shown that the plasma products do not evolve past the electrodes. In addition, in a recent study of solid grains produced in COSmIC from simple hydrocarbon precursors seeded in a Titan-relevant  $N_2$ -based gas carrier, no change in the size of the grains was observed when collecting the grains at two different locations, 5 and 30 cm downstream from the electrodes (Sciamma-O'Brien et al. 2017).

In the study presented here, two solid-phase experiments were run for 3 hours each, to produce cosmic grain analogs from methane (5%) and acetylene (5%) precursors, respectively, seeded in a cold supersonic expansion of argon. Different concentrations of methane were tested in COSmIC, and the 5% concentration was chosen to produce sufficient solid material for analysis in our experimental setup. Methane is a one carbon-atom alkane known to be present in the CSE of carbon-rich stars (Van de Sande & Millar 2019). Acetylene is a two-carbon alkene and the most abundant molecule in the inner region of the CSE where cosmic grains are formed, after  $H_2$  and CO (Fonfria et al. 2008), and is a known precursor of aromatic compounds (Frenklach & Feigelson 1989). For each experiment, chemistry was induced by the plasma discharge through fragmentation and ionization of the molecular precursor and plasma-generated chemical reactions between the precursor, its atomic and molecular fragments, radicals, and ions, resulting in the production of larger molecules and eventually solid particles. The resulting carbon grains, analogs of cosmic dust, were deposited on 3 mm diameter transmission electron microscopy (TEM) copper grids with Ultrathin Carbon Film on Lacey Carbon Support Film (Ted Pella, 400 mesh) placed 3 cm away from the slit, far enough away to avoid

strong disturbances of the expansion. Ultra-high purity (UHP; 99.9998%) Ar and CH<sub>4</sub> gas cylinders were used. The protocol for the addition of C<sub>2</sub>H<sub>2</sub> to the gas mixture using a cold trap has been described in Sciamma-O'Brien et al. (2014). After deposition, the samples were collected under inert argon atmosphere using a custom-made glove box connected to the chamber (see Figure 1), and placed in plastic containers sealed with parafilm to minimize exposure to air before the ex situ analysis of the sample at the SEM facility located at the NASA Ames Advanced Studies Laboratories (Sciamma-O'Brien et al. 2017). The SEM technique was used to characterize the cosmic grain analogs produced in COSmIC. By using the same relative concentration for methane and acetylene (5%), only one experimental parameter (the nature of the precursor) was changed while maintaining all other experimental parameters (energy, temperature, precursor density, and reaction time) identical, thus allowing us to investigate the effect of the molecular precursors (CH<sub>4</sub> versus C<sub>2</sub>H<sub>2</sub>) on the grain size and morphology under controlled conditions.

### 3. Scanning Electron Microscopy Analysis

SEM imaging was performed on a Hitachi S4800 II field emission scanning electron microscope with a 1–2 nm range resolution. The samples were only exposed to ambient air for 1–2 minutes during their transfer to the SEM vacuum chamber for analysis. The settings of the electron beam and optics were varied to obtain the highest-quality images possible for carbon-deposited material on conductive substrates. Electron beam voltages between 10 and 15 kV with a focus current of 7–15  $\mu$ A were used, and the focus/stage distance was set to 8 mm. The current setup of the SEM does not include automated image sampling, and therefore acquisition of images were done manually. The samples were not coated with gold, and as the carbon grains produced in COSmIC are not conductive, they were charging in the electron beam, making it difficult to obtain large quantities of high-quality images. For both gas mixtures, however, we observed enough grains to conduct a statistical analysis of their size distribution. Because many of the grains in the Ar/CH<sub>4</sub> sample and some of the grains in the Ar/C<sub>2</sub>H<sub>2</sub> sample appeared to be nonspherical, we measured, for each grain, the minor and major axes, to be able to quantify the sphericity of the grains and see the effect of the initial gas mixture on their morphology. We also used several images at  $\times 10$  k– $\times 30$  k low magnification (with a resolving power of  $\sim 3$ – $10$  nm/pixel) to conduct particle counting and get the particle density as a function of sample area and the particle production rate as a function of area and time.

#### 3.1. Ar/CH<sub>4</sub> (95:5) Gas Mixture

The SEM images of the sample produced in the Ar/CH<sub>4</sub> (95:5) mixture showed a low density of grains scattered on the lacey carbon film of the TEM copper grid. Figure 2 shows six different  $\times 150$  k– $\times 350$  k high-magnification images of grains observed in this sample, including the largest grain we could observe (bottom center panel). To conduct our statistical analysis, we used two SEM images acquired at  $\times 10$  k– $\times 30$  k low magnification (see Figure 3), i.e., that contained large enough quantities of grains to determine the production rate and size distribution.

One hundred forty-four grains, each made of agglomerates of  $\sim 5$ – $20$  nm size nanoparticles were counted within a total area

of  $54.5 \mu\text{m}^2$ , resulting in an estimated grain density of  $\sim 2.64$  grains  $\mu\text{m}^{-2}$  and a production rate of  $0.88$  grains  $\mu\text{m}^{-2} \text{hr}^{-1}$ . The resolution of these two SEM images was high enough for us to measure the dimensions of the grains using the ImageJ software (Abramoff et al. 2004; see the discussion in Sciamma-O'Brien et al. 2017). Figure 3 shows the resulting grain size distribution, with major axes ranging from 15 nm to as large as 385 nm (very few).

#### 3.2. Ar/C<sub>2</sub>H<sub>2</sub> (95:5) Gas Mixture

The SEM images of the sample produced in the Ar/C<sub>2</sub>H<sub>2</sub> (95:5) mixture showed a higher density of grains scattered on the holey carbon film of the TEM grid than for the sample produced in the Ar/CH<sub>4</sub> (95:5) mixture. Figure 4 shows six different  $\times 80$  k high-magnification images of grains observed in this sample, including the largest grains we could see (top right panel).

As for the Ar/CH<sub>4</sub> (95:5) sample, we conducted a statistical analysis for this sample using two  $\times 10$  k– $\times 30$  k low-magnification SEM images, shown in Figure 5, that contained a sufficiently large quantity of grains and with a high enough spatial resolution ( $< 10$  nm) to measure their dimensions. Three hundred fifty-four grains, each made of agglomerates of  $\sim 5$ – $20$  nm size nanoparticles were counted for a total area of  $101.7 \mu\text{m}^2$ , resulting in an estimated grain density of  $\sim 3.48$  grains  $\mu\text{m}^{-2}$  and a production rate of  $1.16$  grains  $\mu\text{m}^{-2} \text{hr}^{-1}$ . The particle size distribution resulting from this statistical analysis is given in Figure 5. The measured dimensions confirmed what was observed visually, i.e., that the Ar/C<sub>2</sub>H<sub>2</sub> mixture produced larger grains than the Ar/CH<sub>4</sub> mixture, with major axes ranging from 40 nm to as large as 650 nm.

#### 3.3. Sphericity Analysis

When measuring the dimensions of the grains for the Ar/CH<sub>4</sub> and Ar/C<sub>2</sub>H<sub>2</sub> samples, both the minor and major axis dimensions were measured for each grain in order to investigate the sphericity of the grains and the effect of the initial gas composition on their shape. This analysis showed that grains produced in the Ar/CH<sub>4</sub> (95:5) mixture were not only smaller but also less spherical than grains produced in the Ar/C<sub>2</sub>H<sub>2</sub> (95:5) mixture, as shown in Figure 6. On the left-side graphs, the minor versus major axis measurements are plotted for the Ar/CH<sub>4</sub> (red) and Ar/C<sub>2</sub>H<sub>2</sub> (blue) mixtures. Note that the axes are in logarithmic scale. The green diagonal line represents where spherical grains would fall on the plot. The histograms on the right show the frequency of spherical particles for each sample by looking at the ratio between major and minor axis dimensions for each grain.

## 4. Discussion and Conclusions

In COSmIC, we can simulate the processes that occur in the low-temperature outflow of carbon stars and investigate the formation, structure, and size distribution of the cosmic dust grains, which ultimately contribute to the formation of planets. After recently demonstrating that we can use the COSmIC experimental setup to produce cosmic dust analogs at low temperature from gas-phase benzene and PAHs (Gavilan et al. 2020), we have now demonstrated with this study that we can also produce carbonaceous grains starting from small gas-phase hydrocarbon molecules in COSmIC, making this experimental setup the first, to the best of our knowledge, that investigates

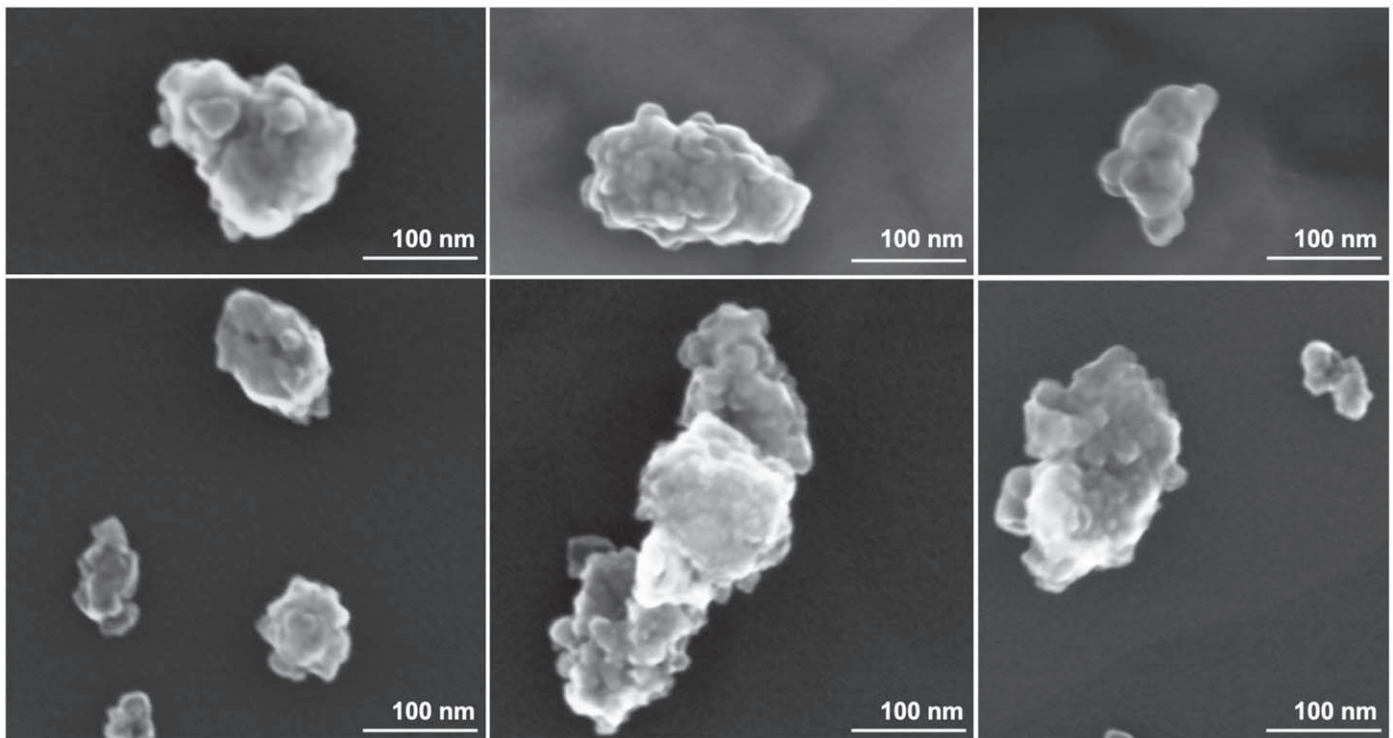


**Figure 2.** High-magnification (150–300 k) SEM images of grains produced in the Ar/CH<sub>4</sub> (95:5) gas mixture with COSmIC (all images have the same scale). All grains were collected in a single run on a TEM copper grid.

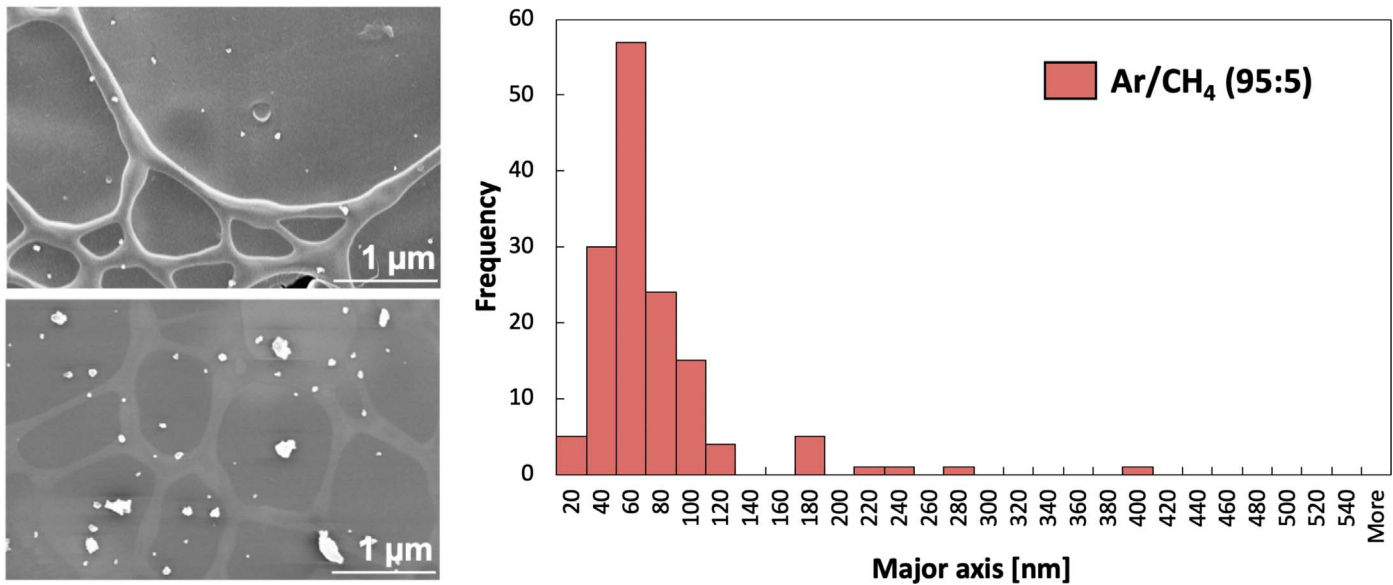


**Figure 3.** Left: low-magnification (10 k, top; 30 k, bottom) SEM images of COSmIC carbonaceous grains produced in the Ar/CH<sub>4</sub> (95:5) gas mixture. Right: particle size distribution resulting from the statistical analysis.

carbon grain formation from the chemical reactions that occur between small gas-phase molecular precursors and their atomic and molecular fragments at low temperature ( $<200$  K) representative of the dust condensation zone and outer region of CSEs. Only one other experimental study of the formation of carbonaceous cosmic grain analogs in the gas phase has been described in the literature (Martínez et al. 2020). In that case, the nanograins were formed from atomic carbon at temperature close to 1000 K simulating the inner CSE.

Previous in situ mass spectrometry characterization of the gas phase in COSmIC have demonstrated that COSmIC's unique design allows us to monitor the different steps in the chemical pathways that lead to the formation of complex molecular species and grains (Contreras & Salama 2013; Sciamma-O'Brien et al. 2014; Raymond et al. 2018). Indeed, because the gas is accelerated to supersonic speed in the expansion generated in the pulsed discharge nozzle (PDN), the residence time of the gas in the plasma cavity is less than  $4 \mu\text{s}$ , which results in a truncated

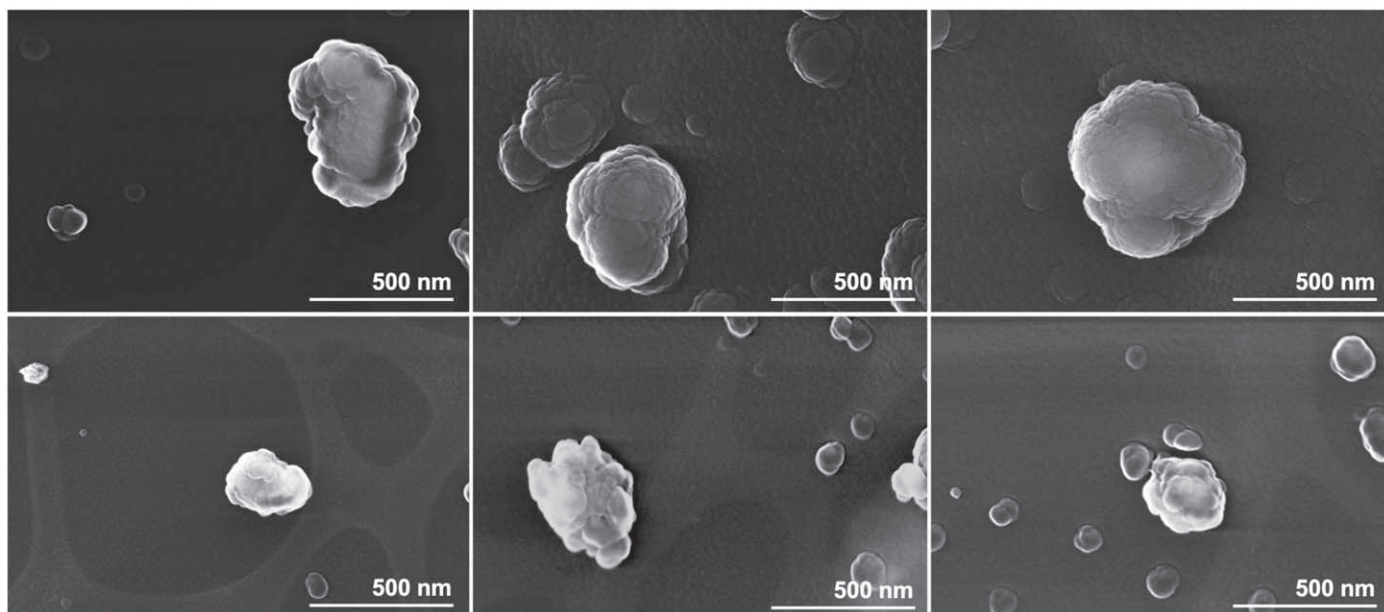


**Figure 4.** High-magnification ( $\times 80$  k) SEM images of grains produced in the Ar/C<sub>2</sub>H<sub>2</sub> (95:5) gas mixture with COSmIC (all images have the same scale). All grains were collected in a single run on a TEM copper grid.

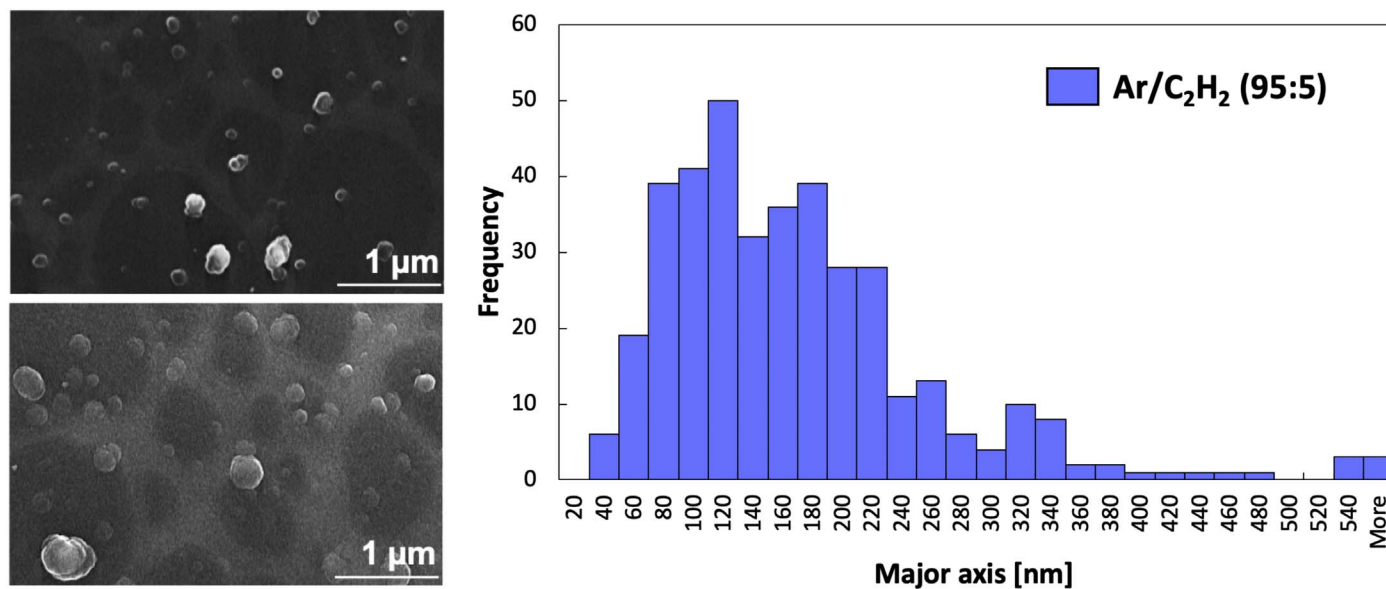


**Figure 5.** Left: low-magnification ( $\times 10$  k) SEM images of COSmIC carbonaceous grains produced in the Ar/C<sub>2</sub>H<sub>2</sub> (95:5) gas mixture. Right: particle size distribution resulting from the statistical analysis.

chemistry enabling us to control how far in the chain of reactions the chemistry is allowed to process. The mass spectrometry studies showed that when heavier precursor molecules were injected in the carrier gas, heavier molecular products were formed in the plasma expansion. It also demonstrated that COSmIC can be used to explore specific chemical pathways by studying the effect of a particular precursor on the chemistry: adding C<sub>2</sub>H<sub>2</sub> in Ar-based and N<sub>2</sub>-based gas mixtures led to the production of benzene in the plasma discharge; and in plasmas generated in gas mixtures containing C<sub>6</sub>H<sub>6</sub>, chemical pathways that support the HACA mechanism for PAH growth through sequential hydrogen abstraction and acetylene (C<sub>2</sub>H<sub>2</sub>) addition were observed (Contreras & Salama 2013; Sciamma-O'Brien et al. 2014). These findings were confirmed by modeling of the experimental system using a one-dimensional model to simulate

and track the evolution of more than 120 species in the plasma, which showed a chemical growth evolution when heavier precursors were present (Raymond et al. 2018).

The SEM study presented here showed that changes in the initial composition of the gas injected in the PDN do influence the morphology and production yield of the cosmic grain analogs produced in COSmIC, which is consistent with the findings in the gas phase. The larger and more spherical shape of the grains produced from the more carbon-rich and more reactive acetylene molecule compared to methane could be explained by going further in the chemistry and producing heavier molecules that contribute to the formation of solid particles (note that the same phenomenon was observed with grains produced from PAH precursors in COSmIC in Gavilan et al. 2020). This is a realistic assumption as the reaction

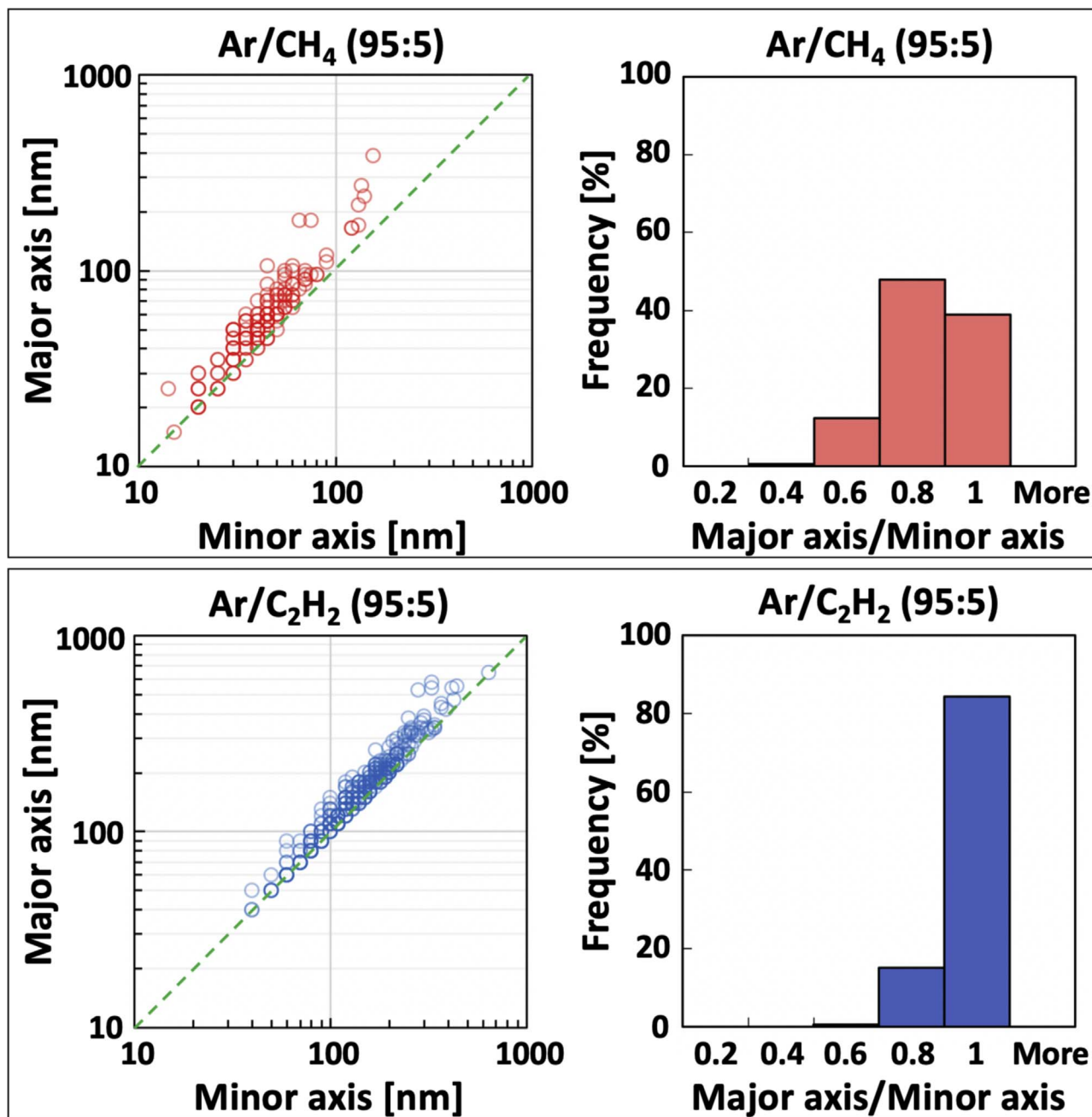


**Figure 6.** Particle sphericity analysis for the Ar/CH<sub>4</sub> (red) and Ar/C<sub>2</sub>H<sub>2</sub> (blue) solid samples. Left: for each sample, the particle sizes are plotted as a function of major and minor axes, confirming that the grains produced in Ar/C<sub>2</sub>H<sub>2</sub> are larger and more spherical than the grains produced in Ar/CH<sub>4</sub>. Right: the histograms show the frequency of sphericity for each sample by considering the major/minor axis ratio.

between the radical C<sub>2</sub>H and C<sub>2</sub>H<sub>2</sub>, one of the simplest neutral-neutral hydrocarbon reactions in chemical models of dense interstellar clouds and carbon-rich circumstellar shells, has a large reaction rate even at low temperature (Herbst & Woon 1997; Agundez & Wakelam 2013). The two types of grains observed in these experiments could then be representative of different stages in the formation of grains: a more “planar” growth at first, followed by coagulation into more spherical particles. This effect has already been observed at higher temperatures in soot formation (Frenklach & Wang 1994; Wang & Abid 2009).

Preliminary energy dispersive X-ray spectroscopy (EDS) analysis of the elemental composition has indicated that carbonaceous grains produced in COSmIC are made of carbon

with a few percent ( $\sim 3\%$ ) of oxygen predominantly due to oxidation during the transfer of the sample into the SEM. Preliminary TEM analysis of our samples has shown that the grains are made of amorphous carbon. Further ex situ analyses that are beyond the scope of the work presented here are being performed and will be discussed in an upcoming paper.

Other experiments have been conducted in plasma environments at room temperature to investigate the formation of carbon grains from small hydrocarbon precursors (e.g., Kovacevic et al. 2005; Peláez et al. 2018), and have led to the formation of amorphous grains with similar sizes and cauliflower shapes to those of the COSmIC grains described here. However, to the best of our knowledge, the COSmIC experiment is the *only* one that is investigating the formation of

carbon grains at low temperature (<200 K). Because the various laboratory experiments that have been developed are conducted under different conditions (temperature, pressure, mixing ratios, energy ...) it is difficult to do a quantitative comparison between experimental results. A more systematic comparative analysis would be very useful in the future to better understand the formation mechanisms by isolating common parameters that lead to similar results from one experiment to another. It is however beyond the scope of this paper.

The SEM study presented here demonstrates the potential of the COSmIC facility to investigate the formation of cosmic grains from gas-phase hydrocarbon precursors at low temperature (<200 K) representative of the dust condensation zone and outer region of CSEs. In addition to pursuing the study of the chemical growth of gas-phase carbon-containing precursors in the CSE environment, this capability opens the door to further analyses of the solid grains such as composition, optical constant determinations, and morphology and structure characterization with IR spectroscopy, SEM, TEM, and Raman spectroscopy, all of which are essential for protoplanetary disk and opacity modeling.

Support from the NASA SMD through an APRA Laboratory Astrophysics Program grant and the NASA Ames Laboratory Astrophysics—the PAH spectroscopic database (and future sister databases) is gratefully acknowledged. The authors recognize the essential contribution of Cesar Contreras to the work presented here. The authors thank Joey Varelas (ASL) for his invaluable help with the characterization of the samples with SEM, and acknowledge fruitful discussions with Ludovic Biennier, Salma Bejaoui, Lisseth Gavilan, Larry Nittler, Rhonda Stroud, Hai Wang, Joe Roser, Andrew Mattioda, and Gustavo Cruz-Diaz. The authors thank Robert Walker and Emmett Quigley for their outstanding technical support.

### ORCID iDs

Ella Sciamma-O'Brien  <https://orcid.org/0000-0002-1883-552X>

Farid Salama  <https://orcid.org/0000-0002-6064-4401>

### References

- Abramoff, M. D., Magalhaes, P. J., & Ram, S. J. 2004, *J. Bio-Photonics Int.*, 11, 36
- Agundez, M., & Wakelam, V. 2013, *ChRv*, 113, 8710
- Allain, T., Sedlmayr, E., & Leach, S. 1997, *A&A*, 323, 163
- Arnas, C., Moberi, A., Hassouni, K., et al. 2009, *JNuM*, 390, 140
- Bejaoui, S., & Salama, F. 2019, *AIPA*, 9, 085021

- Biennier, L., Benidar, A., & Salama, F. 2006, *CP*, 326, 445
- Biennier, L., Georges, R., Chandrasekaran, V., et al. 2009, *Carbon*, 47, 3295
- Biennier, L., Salama, F., Allamandola, L. J., & Scherer, J. J. 2003, *JChPh*, 118, 7863
- Bréchnignac, P., Schmidt, M., Masson, A., et al. 2005, *A&A*, 442, 239
- Broks, B. H. P., Brok, W. J. M., Remy, J., et al. 2005, *PhRvE*, 71, 036409
- Cau, P. 2002, *A&A*, 392, 203
- Cherchneff, I. 2011, in *EAS Pub. Ser. 46, PAHs Universe*, ed. C. Joblin & A. G. G. M. Tielens (Les Ulis: EDP Sciences), 177
- Contreras, C. S., & Salama, F. 2013, *ApJS*, 208, 6
- Contreras, C. S., Sciamma-O'Brien, E., & Salama, F. 2014, *AAS Meeting 224*, 114.04
- Draine, B. T. 2003, *ARA&A*, 41, 241
- Fonfria, J. P., Cernicharo, J., Richter, M. J., & Lacy, J. H. 2008, *ApJ*, 673, 445
- Frenklach, M., & Feigelson, E. 1989, *ApJ*, 341, 372
- Frenklach, M., & Wang, H. 1994, in *Soot Formation in Combustion*, Springer Series in Chemical Physics, Vol. 59, ed. H. Bockhorn (Berlin: Springer), 165
- Fulvio, D., Gobi, S., Jaeger, C., Kereszturi, A., & Henning, T. 2017, *ApJS*, 233, 14
- Gail, H.-P., & Sedlmayr, E. 2013, *Physics and Chemistry of Circumstellar Dust Shells*, Cambridge Astrophysics Series (Cambridge: Cambridge Univ. Press)
- Gavilan, L., Bejaoui, S., Haggmark, M., et al. 2020, *ApJ*, 889, 101
- Henning, T., & Salama, F. 1998, *Sci*, 282, 2204
- Herbst, E., & Woon, D. E. 1997, *ApJ*, 489, 109
- Herpin, F., Goicoechea, J., Pardo, J. R., & Cernicharo, J. 2002, *ApJ*, 577, 961
- Hodoroaba, B., Gerber, I. C., Ciubotaru, D., et al. 2018, *MNRAS*, 481, 2841
- Jäger, C., Huisken, F., Mutschke, H., Jansa, I. L., & Henning, T. 2009, *ApJ*, 696, 706
- Jäger, C., Krasnokutski, S., Staicu, A., et al. 2006, *ApJS*, 166, 557
- Kovacevic, E., Stefanovic, I., Berndt, J., Pendleton, Y. J., & Winter, J. 2005, *ApJ*, 623, 242
- Lee, S., Chen, H.-F., & Chin, C.-J. 2007, *JAP*, 101, 113303
- Martínez, L., Santoro, G., Merino, P., et al. 2020, *NatAs*, 4, 97
- Massalkhi, S., Agúndez, M., & Cernicharo, J. 2019, *A&A*, 628, A62
- NASA Press Release 2014, *NASA Simulator Successfully Recreates Space Dust*, <https://www.nasa.gov/press/2014/may/nasa-simulator-successfully-recreates-space-dust/>
- Peláez, R. J., Maté, B., Tanarro, I., et al. 2018, *PSST*, 27, 035007
- Raymond, A. W., Sciamma-O'Brien, E., Salama, F., & Mazur, E. 2018, *ApJ*, 853, 107
- Ricketts, C. L., Contreras, C. S., Walker, R., & Salama, F. 2011, *IJMSp*, 300, 26
- Salama, F., Galazutdinov, G. A., Krelowski, J., et al. 2011, *ApJ*, 728, 154
- Salama, F., Sciamma-O'Brien, E., Contreras, C. S., & Bejaoui, S. 2017, in *IAU Symp. 332, Astrochemistry VII: Through the Cosmos from Galaxies to Planets*, ed. M. Cunningham, T. Miller, & T. Aikawa (Cambridge: Cambridge Univ. Press), 364
- Sciamma-O'Brien, E., Ricketts, C. L., & Salama, F. 2014, *Icar*, 236, 325
- Sciamma-O'Brien, E., Upton, K. T., Beauchamp, J. L., & Salama, F. 2015, in *IAU Proc. 29A, Astronomy in Focus* (Cambridge: Cambridge Univ. Press), 327
- Sciamma-O'Brien, E., Upton, K. T., & Salama, F. 2017, *Icar*, 289, 214
- Shukla, B., Miyoshi, A., & Koshi, M. 2008, *J. Combust. Soc. Jpn.*, 151, 8
- Tan, X., & Salama, F. 2006, *CPL*, 422, 518
- Van de Sande, M., & Millar, T. J. 2019, *ApJ*, 873, 36
- Wang, H., & Abid, A. D. 2009, in *Combustion Generated Fine Carbonaceous Particles*, ed. H. Bockhorn et al. (Karlsruhe: KIT Scientific Publishing), 367